





TOPICAL REVIEW

Electrophysiology equipment for reliable study of kHz electrical stimulation

Mohamad FallahRad¹, Adantchede Louis Zannou¹ , Niranjan Khadka¹ , Steven A. Prescott^{2,3} , Stéphanie Ratté^{2,3}, Tianhe Zhang⁴, Rosana Esteller⁴, Brad Hershey⁴ and Marom Bikson¹ 

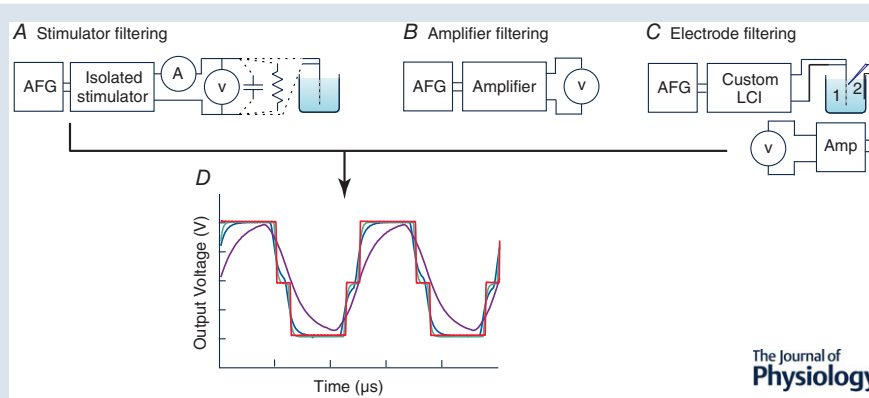
¹Department of Biomedical Engineering, The City College of New York of CUNY, New York, NY, USA

²Neurosciences and Mental Health, The Hospital for Sick Children, Toronto, ON, Canada

³Department of Physiology and Institute of Biomaterials and Biomedical Engineering, University of Toronto, ON, Canada

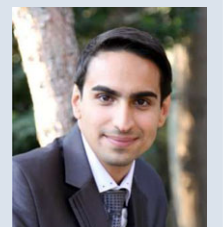
⁴Boston Scientific Neuromodulation, Valencia, CA, USA

Edited by: Ole Petersen & Richard Carson



Abstract Characterizing the cellular targets of kHz (1–10 kHz) electrical stimulation remains a pressing topic in neuromodulation because expanding interest in clinical application of kHz stimulation has surpassed mechanistic understanding. The presumed cellular targets of brain stimulation do not respond to kHz frequencies according to conventional electrophysiology theory. Specifically, the low-pass characteristics of cell membranes are predicted to render kHz stimulation inert, especially given the use of limited-duty-cycle biphasic pulses. Precisely because kHz frequencies are considered supra-physiological, conventional instruments designed for neurophysiological studies such as stimulators, amplifiers and recording microelectrodes do not operate reliably at these high rates. Moreover, for pulsed waveforms, the signal frequency content is well above the pulse repetition rate. Thus, the very tools used to characterize the effects of kHz electrical stimulation may themselves be confounding factors. We illustrate custom equipment design that supports reliable electrophysiological recording during kHz-rate stimulation. Given the increased importance of kHz stimulation in clinical domains and compelling possibilities that

Mohamad FallahRad received the Master of Science degree in computer engineering from the Iran University of Science and Technology, in 2012. He worked at Zahn Innovation Center of New York in assisting startup projects with potential funding. He is a lead hardware and software developer at the neural engineering laboratory (BME) of the City College of New York. His long-established research activities are in the fields of current control stimulators and electroporator for human and animal studies.



mechanisms of actions may reflect yet undiscovered neurophysiological phenomena, attention to suitable performance of electrophysiological equipment is pivotal.

(Resubmitted 11 January 2019; accepted after revision 19 February 2019; first published online 28 February 2019)

Corresponding author M. Bikson: Department of Biomedical Engineering, The City College of New York of CUNY, NY, USA. Email: bikson@ccny.cuny.edu

Abstract figure legend Signal filtering (attenuation) caused by electrophysiology devices. *A*, illustration of the performance of an isolator during kHz pulsed stimulation verified using a resistive, capacitive or electrode (non-linear) load and high precision ammeter and voltmeter. *B*, amplifier performance (in response to 1 mV sinusoidal input). *C*, experimental testing of attenuation with frequency by applying sinusoidal current to an experimental lead in a saline bath and measuring voltage. *D*, significant waveform distortion (below 100 kHz) from conventional stimulator and isolator, amplifier, and microelectrode (*A–C*), which can only be corrected by custom circuitry here.

Promise and pitfalls of kHz stimulation

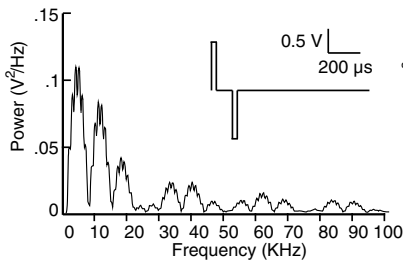
High rate stimulation at frequencies ≥ 1 kHz is of growing interest in neuromodulation because of physiological and clinical features that imply mechanisms beyond those implicated in conventional (<100 Hz) neurostimulation (Kilgore *et al.* 2004; Ward, 2009; Grossman *et al.* 2017; Thomson *et al.* 2018; Noori & Mehta, 2018). Yet, how neurons respond to kHz frequencies remains an open question (Pelot *et al.* 2017; Crosby *et al.* 2017; Dmochowski and Bikson, 2017; Li *et al.* 2018; Zannou *et al.* 2019). The development of kHz stimulation techniques and their characterization requires suitable electrophysiological equipment, but as we show here, conventional electrophysiology technology is not designed to handle such high frequencies and may not function reliably. For pulsed stimulation at kHz rates, the decreasing periods (inter-pulse times) require decreases in pulse width, which results in signals with frequency content (Fig. 1Aa and b) that violate the specifications for conventional research-grade electrophysiology stimulators, amplifiers and electrodes. We first show that conventional stimulation voltage-to-current isolators do not support generation of such waveforms and can introduce bias; to address this, we propose an isolator circuit with >100 kHz bandwidth. In addition, conventional electrophysiology amplifiers include filter limitations based on conventional neurophysiological bandwidths; to address this, we propose an instrumentation amplifier circuit with >100 kHz bandwidth. Finally, we show that both glass and metal recording microelectrodes act as low-pass filters; depending upon experimental design, this may confound recordings of responses caused by >1 kHz stimulation, which is a pitfall that is not readily addressable since it stems from properties inherent to the electrode material. Careful verification of any equipment used to characterize the effects of kHz stimulation is necessary to ensure the reliability of electrophysiological results.

Attenuation of kHz frequencies by conventional and custom stimulation isolators

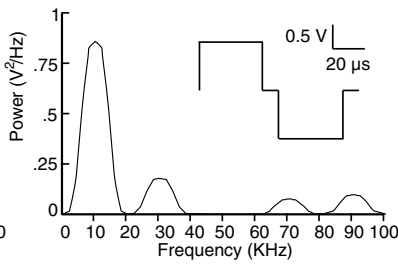
For flexible experimentation, the use of voltage-to-current isolators theoretically allows application of a wide range of controlled waveforms compared to specialized pulse generators (e.g. clinical implantable pulse generators); but the utility of isolators depends on providing non-distorted kHz waveforms (Patel & Butera, 2018). In addition to testing three commercial isolators, we implemented our own high-bandwidth linear current isolator (LCI) design as described.

Arbitrary voltage waveforms are generated by a function generator (digital to analog converters, D/A) and an ideal isolator would faithfully convert this command voltage to a current signal across appropriate loads. However, using a resistive test load (Fig. 1Ba), three common commercially available isolators (SRS CS580, Stanford Research Systems, Sunnyvale, CA, USA; A-M Systems 2200, A-M Systems, Sequim, WA, USA; WPI A395, World Precision Instruments, Sarasota, FL, USA) produced unintended waveform attenuation and distortion at higher kHz frequencies. First, the output voltage across the $1\text{ k}\Omega$ resistive load was measured using a sinusoidal voltage command at frequencies of 1 Hz and 10–100 kHz; the voltage output peak at each frequency, normalized (%) to the peak at 1 Hz, provides the linear transfer function of the isolators (Fig. 1Bc). A decrease in normalized output peak at higher frequencies reflects bandwidth filtering, with only the LCI output not attenuated at frequencies >30 kHz. Second, isolator output was measured during biphasic rectangular symmetric pulsed voltage command at 1 kHz (40 μs pulse duration, 100 μs inter-pulse) and 10 kHz (40 μs pulse duration, 10 μs inter-pulse). Bandwidth limitations are then reflected in the fidelity of pulse generation over resistive load (Fig. 1Bd and e). Pulse outputs were attenuated (limited rise time) for all tested isolators except the LCI. Additional testing under a

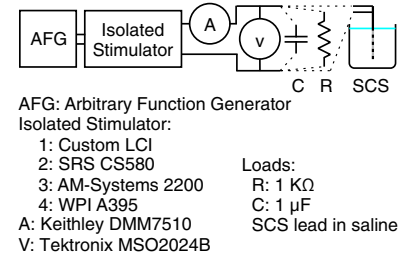
Aa Frequency content of 1 kHz biphasic



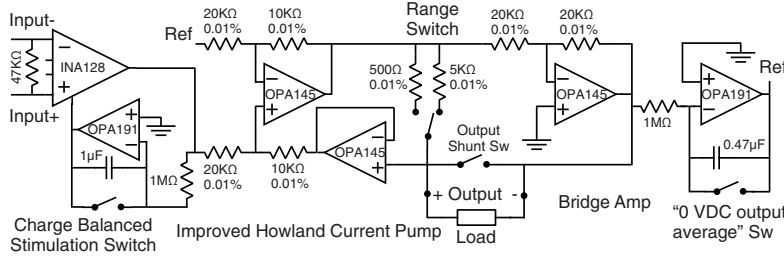
Ab Frequency content of 10 kHz biphasic



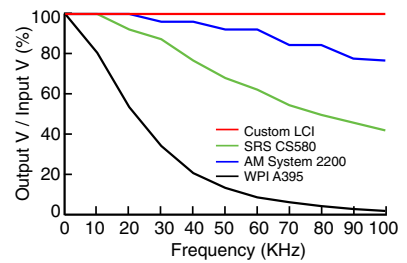
Ba Stimulator test setup (different loads)



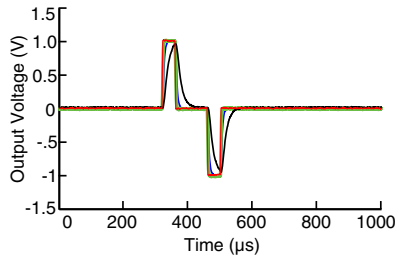
Bb Custom Linear Current Stimulator



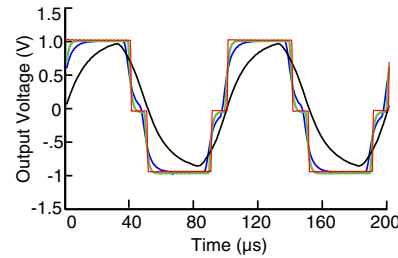
Bc Stimulator attenuation



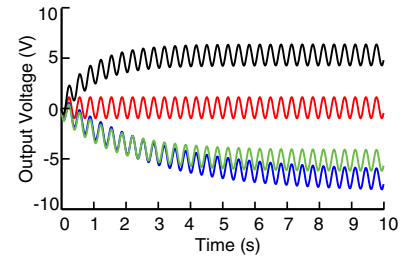
Bd 1 KHz biphasic 1 mA across 1 KΩ



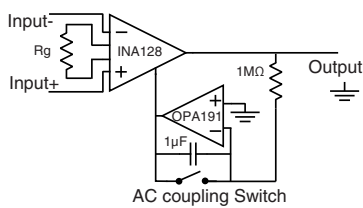
Be 10 KHz biphasic 1 mA across 1 KΩ



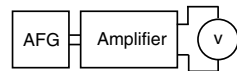
Bf 3 Hz sine 2 mApp across 1 µF



Ca Custom amplifier

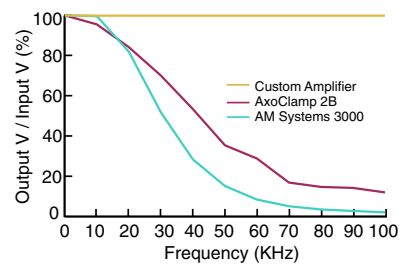


Cb Amplifier test setup

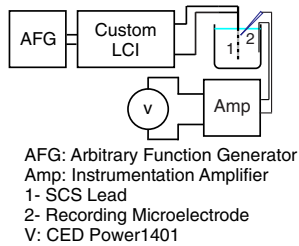


AFG: Arbitrary Function Generator
 Amplifier:
 1: Custom Amplifier
 2: Axoclamp 2B
 3: AM-Systems 3000
 V: CED Power1401

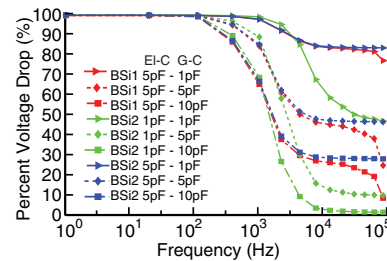
Cc Amplifier attenuation



Da Electrode test setup



Db Glass electrodes simulation



Dc Metal/Glass electrodes experiment

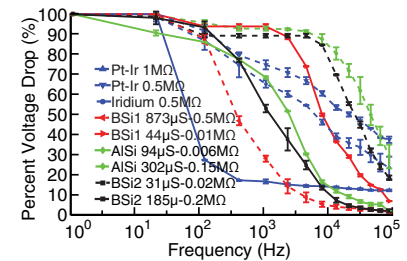


Figure 1. Attenuation over frequency for stimulation isolators, amplifiers and microelectrodes
 kHz pulsed stimulation has broad-band frequency content including symmetric biphasic 1 kHz (Aa) and 10 kHz (Ab) waveforms. Isolator performance can be verified using a resistive, capacitive or electrode (non-linear) load and high precision current and voltage meters (Ba). In addition to three commercial isolators (SRS CS580, A-M

capacitive load (Fig. 1*Bf*) revealed isolator DC bias, which can further undermine experiments (Franke *et al.* 2014).

We overcome these issues with a custom open-source LCI (Fig. 1*Bb*) capable of reliably delivering waveforms with frequency content up to 100 kHz (Fig. 1*Bc*). The input stage is implemented using an instrumentation amplifier (INA128U, Texas Instruments, Dallas, TX, USA), for limiting the current to the stimulator to 2 nA and eliminating the loop current. Maximum gain error of the INA128U is 0.01%, with non-linearity of 0.001%, and the maximum output offset voltage is 50 μ V (post-gain); for extracellular recordings this DC offset can be filtered. The circuit is based on an improved Howland current pump with bridge output and floating load. The voltage to current converter is implemented using an operational amplifier (OPA145, Texas Instruments) and 0.01% 1/4 W precision resistors. The OPA145 shows 40 μ V of offset, open loop gain of 123 dB and gain bandwidth product of 5.5 MHz. The compliance voltage of the isolator is about ± 36 V with the input range of ± 10 V and output impedance of 30 M Ω . Linear accuracy of the isolator is 0.01%, with two selectable ranges of 100 μ A/V and 1 mA/V with the feedback resistor value of 500 Ω and 5 k Ω , respectively. The isolator has two additional features to minimize potential for even a small undesired DC current (Kilgore and Bhadra, 2004; Merrill *et al.* 2005) during precise neurostimulation experiments: (1) optional removal of the input DC offset for accurate charge balanced stimulation, and (2) selectable elimination of DC bias of output (AC coupling) by setting the negative output voltage integration as reference of the Howland current pump. The time constant of the integrator is high and as a result the output waveform matches the input waveform with high fidelity. The power source of the LCI consists of three Li-ion cells in series, each with 3400 mAh capacity, battery protection circuitry, charge circuitry, and a dual output DC/DC boost converter followed by passive filters and accurate linear low dropout (LDO) regulators.

Finally, testing the experiment-specific electrode system (e.g. an experimental spinal cord stimulation (SCS) lead in saline; Fig. 1*Bb*) addresses issues arising from non-linear electrode impedance (Merrill *et al.* 2005). For such verifications, measurement of both output current and voltage using high resolution and temporal precision meters is recommended (e.g. Keithley DMM7510, Tektronix, Beaverton, OR, USA; MSO2024B, Tektronix; Fig. 1*Ba*), noting that current/voltage may become dissociated with complex electrode loads (Merrill *et al.* 2005). The custom LCI, but not commercial isolators, supports kHz pulsed stimulation across electrode loads (not shown). Thus, specially designed isolators or specialized pulse generators are required for reliable kHz stimulation.

Attenuation over kHz frequency of conventional and custom amplifiers

Low-pass filtering is inherent to the design of electrophysiology amplifiers, with bandwidths limited by the frequencies expected in neurophysiological signals. We tested two conventional electrophysiology amplifiers (Axoclamp 2B, Axon Instruments, Union City, CA, USA; and A-M Systems 3000) by directly applying sinusoidal signals from a function generator (Tektronix AFG1022) (Fig. 1*Cb*) and observed low-pass properties consistent with manufacturer specifications and without significant non-linear distortion (Fig. 1*Cc*). Nevertheless, the measured cut-offs were below the bandwidth of the frequency content of kHz pulsed stimulation waveforms. The commercial amplifiers tested here linearly attenuated the signals, which is 'passable' performance during kHz stimulation depending on the experimental design; for example, performance was sufficient for measuring spiking rate but not for calibrating electric field intensity. Especially, given increasing electrophysiology amplifier

Systems 2200, WPI A395) we designed a specialized isolator circuit (*Bb*). Each stimulation isolator output over frequency was tested using a sinusoidal 1 V peak command and a 1 k Ω load, with all but the custom isolator showing significant attenuation with frequencies below 100 kHz (*Bc*). A command intended to produce a 1 kHz (*Bd*) or 10 kHz (*Be*) 1 mA pulse across a 1 k Ω load shows significant waveform distortion for all amplifiers except the custom circuit. A sinusoidal command applied to isolators connected to a capacitive load demonstrated a DC offset in the commercial but not custom isolators. To evaluate amplifier performance, a basic amplifier circuit (*Ca*) and two electrophysiology amplifiers (Axoclamp 2B, A-M Systems 3000) outputs were measured in response to a 1 mV sinusoidal input (*Cb*). The electrophysiology amplifiers but not the custom amplifier exhibited significant frequency attenuation below 100 kHz (*Cc*). Finally, attenuation with frequency by microelectrodes was tested by applying sinusoidal current (using the custom isolator) to an experimental lead in a saline bath and measuring voltage (using the custom amplifier) (*Da*) for various types of glass and metal microelectrodes, and simulated using a lumped element model. (*Dc*). Two types of borosilicate glass pipette electrodes were modeled (BSi1 and BSi2) varying ground-coupling (G-C) and electrode interface-coupling (EI-C) capacitances. (*Db*). Three types of metal electrodes (Pt-Ir and Ir) and six types of glass electrodes (BSi1, BSi2 and AlSi) were experimentally tested. All results showed electrode types-specific attenuation with high cut-offs frequencies of 0.1–10 kHz. This analysis demonstrates frequency attenuation with conventional stimulation and isolators and amplifiers, which can be overcome with dedicated circuit design, while microelectrode attenuation results from the physical properties of the electrode and can be measured.

complexity, there is an increasing risk of distortion (see below).

In contrast, a simple low-cost instrumentation amplifier circuit (Fig. 1Ca) provided a nearly flat frequency response with 0.05% gain non-linearity (Fig. 1Cc), a common mode rejection ratio of 120 dB and -3 dB bandwidth of 200 kHz at gain of 100. The instrumentation amplifier is battery powered and has ultra-low noise with low-frequency noise of $\sim 0.2 \mu\text{V}_{\text{peak-to-peak}}$ measured from 0.1 to 10 Hz. The amplifier is designed with a minimum number of components, low power consumption (1.8 mA total quiescent current), selectable gain, AC and DC coupling, and a battery indicator. The amplifier maximum offset voltage is $50 \mu\text{V}$. The input has maximum 5 nA of input bias current and $10 \text{ G}\Omega$ of impedance. Thus, simple circuits may be useful for high input-impedance amplification in kHz electrical stimulation studies.

When patch clamp amplifiers designed for voltage clamp recordings (like the Axoclamp 200B) are used in current clamp mode, the large voltage signal caused by electrical stimulation causes the amplifier to inject a corrective current into the patched cell (Magistretti *et al.* 1996; Lesperance *et al.* 2018). In this scenario, the cell voltage is inadvertently altered by the recording equipment rather than simply being mis-measured. Compounding this, small perturbations in cell voltage might dissipate if perturbations occurred at low rate, but when stimulating at high rate (i.e. kHz), perturbations summate and fundamentally compromise the experiment (Lesperance *et al.* 2018). This artifactual current injection does not occur with true voltage-follower amplifiers (e.g. Axoclamp 2B), but with new generations of electrophysiologists growing less familiar with amplifier design and more reliant on software to automate amplifier settings (e.g. capacitance compensation during patch clamp recording), there is an increasing risk not only that anomalies arise, but also they go unnoticed.

Attenuation over kHz frequency by microelectrodes

Microelectrodes are ubiquitous for the characterization of electrophysiological responses at the small network and cellular level. During electrical stimulation studies, electrodes serve two functions: (1) to verify (calibrate) the electric field produced by stimulation, and (2) to measure neurophysiological responses. To test for any filtering by microelectrodes, we generated sinusoidal current using the LCI isolator, passed across bipolar electrodes (cylindrical polyurethane lead, platinum/iridium electrode contacts, 1.35 mm electrode diameter, 3 mm electrode length, 1 mm inter-electrode spacing) in a saline bath (Fig. 1Da), while measuring the voltage ~ 1 cm from the bipolar electrode with a microelectrode using an instrumentation amplifier. The LCI isolator and instrumentation amplifier have

bandwidth over the frequencies tested (<100 kHz), and no frequency attenuation is expected across the saline bath (quasi-static at kHz frequencies; Cook, 1991); therefore, we presume any decrease in voltage with increasing frequency (normalize to voltage at 1 Hz) measured by the test system reflects (low-pass) filtering by the microelectrode. Moreover, testing multiple microelectrodes supported the hypothesis that filtering is related to microelectrode specific materials. We considered borosilicate (BSi) and aluminosilicate (AlSi) glass microelectrodes and platinum-iridium (Pt-Ir) and iridium (Ir) metal electrodes (Fig. 1Dc). In addition, electrode filtering was simulated with a lumped element computational model (LTSPICE, Analog Devices, Norwood, MA, USA) consisting of two parallel resistor-capacitor (RC) filters (corresponding to the electrode shaft and tip) with varied capacitance (Fig. 1Db) in parallel with the amplifier input (e.g. parasitic capacitance to amplifier ground). Two borosilicate glass pipette electrodes were modelled (BSi1 and BSi2). Electrode interface coupling (EI-C) capacitance was fixed to 5 pF for BSi1 and to either 1 pF or 5 pF for BSi2. Ground coupling (G-C) capacitance values of 1, 5 or 10 pF were associated with each EI-C value of the glass pipette electrodes. For experiment and simulations, voltage values were recorded as a function of the stimulation frequencies (from 1 Hz to 100 kHz), normalized to 1 Hz.

All microelectrodes tested at kHz rates exhibited low-pass filtering that attenuates the signal in an electrode material-specific manner (Fig. 1Db and c). The filtering was consistent with tip resistance, shaft resistance and shaft capacitance of the circuit network. It correlated with the microelectrode transfer function (time constant) as independently measured by current injection through the amplifier while using the electrode-specific models (not shown). The electrode filtering was independent but would be superimposed on any amplifier attenuation. In the case of patch clamp amplifiers (see above), the capacitance of the glass pipette was also shown to affect the amplitude of the distortion and, in turn, affect the total magnitude of the artifactual current injected into the patched cell (Lesperance *et al.* 2018). In that example, both the electrode and the amplifier properties had to be considered in order to fully account for the artifact. The ramifications of microelectrode filtering are experiment specific, unavoidably confounding electric field calibration and potentially compromising the neurophysiological recordings (depending on amplifier specifics) as described.

Conclusions and recommendations

The value of characterizing the effects of kHz electrical stimulation on neurophysiology is increasingly recognized, even as key mechanistic puzzles emerge. In studies on the electrophysiological effects of kHz

stimulation, conventional hardware cannot be used without consideration of equipment performance in the context of experimental design and outcome measures. The frequency attenuation of amplifiers, isolators and electrodes marketed for electrophysiology reflects the input characteristics for which these devices were designed. It is not a design fault, but rather a limitation that electrophysiologists who work with kHz frequency stimulation need to be aware of. Stimulator and amplifier attenuation can be overcome by specialized circuitry as described here. In the case of stimulation isolators, the cost of attenuation reflects the extent that the details of stimulation waveform (e.g. presence of higher frequency components, total charge) influence neurophysiological response (Song *et al.* 2015; Patel & Butera, 2018); or if isolators distortion is not-linear (e.g. low frequency content is introduced) the experiment may be fundamentally compromised (Franke *et al.* 2014; Kasten *et al.* 2018). In the case of amplifiers and electrodes, the cost of band-width limits will reflect the experimental design. When used for voltage field calibration, amplifier and electrode attenuation is problematic, including with sub-kHz pulses since they have kHz frequency content (Miocinovic *et al.* 2009). Amplifier and electrode attenuation may not be critical for conventional neurophysiological measures (e.g. action potential threshold or rate, low frequency oscillation power; Grossman *et al.* 2017; Negahbani *et al.* 2018) unless (1) stimulation artifact removal depends on accurate field pick-up (Helfrich *et al.* 2014; Dowsett and Herrmann 2016); (2) when recording hardware non-linearities are of concern (Lesperance *et al.* 2018; Kasten *et al.* 2018); (3) when electrophysiological responses at kHz rate (e.g. kHz fluctuations in membrane potential) are of interest (Pelot *et al.* 2017); and (4) when interactions between equipment and the body introduce complex distortions (Neuling *et al.* 2017; Noury and Siegel, 2018; Gebodh *et al.* 2019).

References

- Cook O (1991). Radio frequency attenuation of saline solutions. *IEEE 1991 International Symposium on Electromagnetic Compatibility*, pp. 182–183. <https://doi.org/10.1109/ISEMC.1991.148209>
- Crosby ND, Janik JJ & Grill WM (2017). Modulation of activity and conduction in single dorsal column axons by kilohertz-frequency spinal cord stimulation. *J Neurophysiol* **117**, 136–147.
- Dmochowski J & Bikson M (2017). Noninvasive neuromodulation goes deep. *Cell* **169**, 977–978.
- Dowsett J & Herrmann CS (2016). Transcranial alternating current stimulation with sawtooth waves: Simultaneous stimulation and EEG recording. *Front Hum Neurosci* **10**, 135.
- Franke M, Bhadra N, Bhadra N & Kilgore K (2014). Direct current contamination of kilohertz frequency alternating current waveforms. *J Neurosci Methods* **232**, 74–83.
- Gebodh N, Esmaeilpour Z, Adair D, Chelette K, Dmochowski J, Woods AJ, Kappenman ES, Parra LC & Bikson M (2019). Inherent physiological artifacts in EEG during TDCS. *Neuroimage* **185**, 408–424.
- Grossman N, Bono D, Dedic N, Kodandaramaiah SB, Rudenko A, Suk H-J, Cassara AM, Neufeld E, Kuster N, Tsai LH, Pascual-Leone A & Boyden ES (2017). Noninvasive deep brain stimulation via temporally interfering electric fields. *Cell* **169**, 1029–1041.e16.
- Helfrich RF, Knepper H, Nolte G, Strüber D, Rach S, Herrmann CS, Schneider TR & Engel AK. (2014). Selective modulation of interhemispheric functional connectivity by HD-TACS shapes perception. *PLoS Biol* **12**, e1002031.
- Kasten FH, Negahbani E, Fröhlich F & Herrmann CS (2018). Non-linear transfer characteristics of stimulation and recording hardware account for spurious low-frequency artifacts during Amplitude Modulated Transcranial Alternating Current Stimulation (AM-TACS). *Neuroimage* **179**, 134–143.
- Kilgore KL & Bhadra N (2004). Nerve conduction block utilising high-frequency alternating current. *Med Biol Eng Comput* **42**, 394–406.
- Lesperance LS, Lankarany M, Zhang TC, Esteller R, Ratté S & Prescott SA (2018). Artfactual hyperpolarization during extracellular electrical stimulation: Proposed mechanism of high-rate neuromodulation disproved. *Brain Stimul* **11**, 582–591.
- Li S, Farber JP, Linderoth B, Chen J & Foreman RD (2018). Spinal cord stimulation with ‘Conventional Clinical’ and higher frequencies on activity and responses of spinal neurons to noxious stimuli: An animal study. *Neuromodulation* **21**, 440–447.
- Magistretti J, Mantegazza M, Guatteo E & Wanke E (1996). Action potentials recorded with patch-clamp amplifiers: Are they genuine? *Trends Neurosci* **19**, 530–534.
- Merrill DR, Bikson M & Jefferys JGR (2005). Electrical stimulation of excitable tissue: Design of efficacious and safe protocols. *J Neurosci Methods* **141**, 171–198.
- Miocinovic S, Lempka SF, Russo GS, Maks CB, Butson C, Sakaie KE, Vitek Jerrold L, McIntyre CC (2009). Experimental and theoretical characterization of the voltage distribution generated by deep brain stimulation. *Exp Neurol* **215**, 166–176.
- Negahbani E, Kasten FH, Herrmann CS & Fröhlich F (2018). Targeting alpha-band oscillations in a cortical model with amplitude-modulated high-frequency transcranial electric stimulation. *Neuroimage* **173**, 3–12.
- Neuling T, Ruhnau P, Weisz N, Herrmann CS & Demarchi G (2017). Faith and oscillations recovered: On analyzing EEG/MEG signals during TACS. *Neuroimage* **147**, 960–963.
- Noori S & Mehta N (2018). Management of medically refractory central poststroke pain using high-frequency spinal cord stimulation at 10 kHz. *Neuromodulation* **21**, 823–825.
- Noury N & Siegel M (2018). Analyzing EEG and MEG signals recorded during TES, a reply. *Neuroimage* **167**, 53–61.
- O’Keeffe DT, Lyons GM, Donnelly AE & Byrne CA (2001). Stimulus artifact removal using a software-based two-stage peak detection algorithm. *J Neurosci Methods* **109**, 137–145.

- Patel YA & Butera RJ (2018). Challenges associated with nerve conduction block using kilohertz electrical stimulation. *J Neural Eng* **15**, 031002.
- Pelot NA, Behrend CE & Grill WM (2017). Modeling the response of small myelinated axons in a compound nerve to kilohertz frequency signals. *J Neural Eng* **14**, 046022.
- Song Z, Meyerson BA & Linderoth B (2015). High-frequency (1 kHz) spinal cord stimulation-is pulse shape crucial for the efficacy? A pilot study. *Neuromodulation* **18**, 714–720.
- Thomson SJ, Tavakkolizadeh M, Love-Jones S, Patel NK, Gu JW, Bains A, Doan Q & Moffitt M (2018). Effects of rate on analgesia in kilohertz frequency spinal cord stimulation: Results of the PROCO randomized controlled trial. *Neuromodulation* **21**, 67–76.
- Ward AR (2009). Electrical stimulation using kilohertz-frequency alternating current. *Phys Ther* **89**, 181–190.
- Zannou AL, Khadka N, Truong DQ, Zhang T, Esteller R, Hershey B & Bikson M (2019). Temperature increases by kilohertz frequency spinal cord stimulation. *Brain Stimul* **12**, 62–72.

Additional information

Competing interests

The City University of New York (CUNY) has intellectual property (IP) on neuro-stimulation system and methods with authors N.K. and M.B. as inventors. S.A.P. serves on the Scientific Advisory Board for Boston Scientific and has received research

funding from Boston Scientific. M.B. has equity in Soterix Medical Inc. and serves as an advisor of Boston Scientific Inc. and GlaxoSmithKline. T.Z., R.E. and B.H. are employees of Boston Scientific Inc.

Author contributions

M.F. acquired and analysed the data, and drafted the manuscript. A.L.Z. acquired and analysed the data and drafted the manuscript. N.K. drafted, edited and revised the manuscript. S.A.P., S.R., T.Z., R.E. and B.H. revised the manuscript and provided intellectual content. M.B. designed the work, drafted the manuscript, and revised it for important intellectual content. All authors have read and approved the final version of this manuscript and agree to be accountable for all aspects of the work in ensuring that questions related to the accuracy or integrity of any part of the work are appropriately investigated and resolved. All persons designated as authors qualify for authorship, and all those who qualify for authorship are listed.

Funding

This study was partially funded by grants to M.B. from NIH (NIH-NIMH1R01MH111896, NIH-NINDS1R01NS101362, NIH-NCIU54CA137788/U54CA132378, R03NS054783), New York State Department of Health (NYS DOH, DOH01-C31291GG), and Boston Scientific Inc. (ISRNON60014).